Resistance oscillations of two-dimensional electrons in crossed electric and tilted magnetic fields

William Mayer and Sergey Vitkalov*
Physics Department, City College of the City University of New York, New York, New York 10031, USA

A. A. Bykov
A. V. Rzhanov Institute of Semiconductor Physics, Novosibirsk 630090, Russia
and Novosibirsk State University, Novosibirsk 630090, Russia

(Received 28 March 2016; published 28 June 2016)

The effect of dc electric field on transport of highly mobile two-dimensional electrons is studied in wide GaAs single quantum wells placed in titled magnetic fields. The study shows that in perpendicular magnetic field resistance oscillates due to electric-field induced Landau-Zener transitions between quantum levels that correspond to geometric resonances between cyclotron orbits and periodic modulation of electron density of states. Magnetic field tilt inverts these oscillations. Surprisingly the strongest inverted oscillations are observed at a tilt corresponding to nearly absent modulation of the electron density of states in regime of magnetic breakdown of semiclassical electron orbits. This phenomenon establishes an example of quantum resistance oscillations due to Landau quantization, which occur in electron systems with a *constant* density of states.

DOI: 10.1103/PhysRevB.93.245436

The quantization of electron motion in magnetic fields generates a great variety of fascinating transport phenomena observed in condensed materials. Shubnikov-de Haas (SdH) resistance oscillations [1] and quantum Hall effect [2] are famous examples related to the linear response of electrons. Finite electric fields produce remarkable nonlinear effects. At small electric fields Joule heating strongly modifies the two-dimensional (2D) electron transport [3–6], yielding exotic electronic states in which voltage (current) does not depend on current [7–9] (voltage [10]). Application of a stronger electric field E produces spectacular resistance oscillations [11–16]. The oscillations are periodic with the electric field and obey the following relation:

$$\gamma e R_c E = j\hbar\omega_c, \tag{1}$$

where e is electron charge, R_c is the radius of cyclotron orbits of electrons at Fermi energy E_F, j is a positive integer, and factor $\gamma \approx 2$. These oscillations are related to impurity assisted Landau-Zener transitions between Landau levels titled by the electric field [11] and can be treated as geometrical resonances between cyclotron orbits and spatially modulated density of states [17,18].

Two-dimensional electron systems with multiple populated sub-bands exhibit additional quantum magnetoresistance oscillations [19–26]. These magneto-inter-sub-band oscillations (MISO) are due to an alignment between Landau levels from different sub-bands i and j with corresponding bottom energies E_i and E_j. The level alignment produces resistance maximums at the condition

$$\Delta_{ij} = k\hbar\omega_c, \tag{2}$$

where $\Delta_{ij} = E_j - E_i$ and the index k is a positive integer [27–30]. At a half integer k Eq. (2) corresponds to resistance minimums occurring at nearly constant density of states (DOS) for broad levels [29,30].

An application of in-plane magnetic field to the multi-sub-band systems creates significant modifications of electron spectra leading to a fascinating beating pattern of SdH oscillations and magnetic breakdown of semiclassical orbits [31–37]. Recently it was shown that MISO are strongly modified by the in-plane magnetic field, leading to a spectacular collapse of the beating nodes due to magnetic breakdown [40].

In this paper we present investigations of the effect of the electric field on electron transport in three-sub-band electron systems placed in tilted magnetic fields. The study reveals that the in-plane magnetic field inverts the electric-field induced resistance oscillations described by Eq. (1). The strongest inverted oscillations are observed at the high-frequency (HF)-MISO nodes in the regime of magnetic breakdown, in the *absence* of the modulations of the density of states at the fundamental frequency $1/\hbar\omega_c$. At these conditions the dissipative resistance reaches a minimum value, which is smaller than the resistance at zero magnetic field.

A selectively doped GaAs single quantum well of width $d = 56$ nm was grown by molecular-beam epitaxy on a semi-insulating (001) GaAs substrate. The heterostructure has three populated sub-bands with energies $E_1 \approx E_2 << E_3$ at the bottoms of the sub-bands. The energy diagram is schematically shown in the inset to Fig. 1. Hall bars with width $W = 50\,\mu$m (y direction) and distance $L = 250\,\mu$m (x direction) between potential contacts demonstrating electron mobility $\mu \approx 1.6 \times 10^6$ cm^2/V s and total density $n_T = 8.8 \times 10^{15}$ m^{-2} were studied at temperature 4.2 K. The magnetic field, $\vec{B}$, was directed at different angles α relative to normal to the samples and perpendicular to the electric current. Hall resistance $R_H = B_\perp/(en_T)$ yields the angle α, where $B_\perp = B\cos(\alpha)$ is the perpendicular magnetic field. Current $I_{\rm ac} = 1\,\mu$A at 133 Hz was applied through the current contacts and the longitudinal and Hall ac voltages ($V_{xx}^{\rm ac}$ and $V_H^{\rm ac}$) were measured in response to a variable dc bias $I_{\rm dc}$ applied through the same current leads. The measurements were done in the linear regime in which the ac voltages are proportional to $I_{\rm ac}$, yielding differential resistance $r_{xx}(I_{\rm dc}) = V_{xx}^{\rm ac}/I_{\rm ac}$. Samples A

*Corresponding author: vitkalov@sci.ccny.cuny.edu

 ©2016 American Physical Society

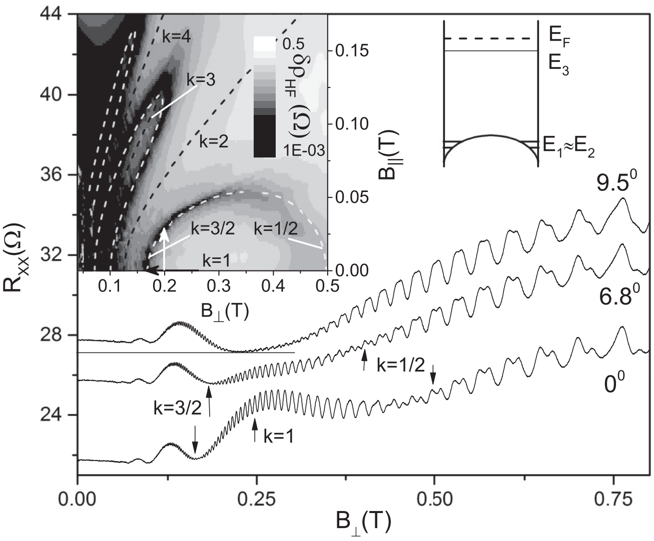

FIG. 1. Dependence of dissipative resistance on perpendicular magnetic field at different angles α as labeled. Curves are shifted for clarity. The right inset presents an energy diagram of studied samples. The left inset presents the magnitude of HF-MISO in the $B_\perp - B_\parallel$ plane. White (black) dashed lines present expected positions of HF-MISO nodes (LF-MISO maximums) obtained numerically [40]. Sample A.

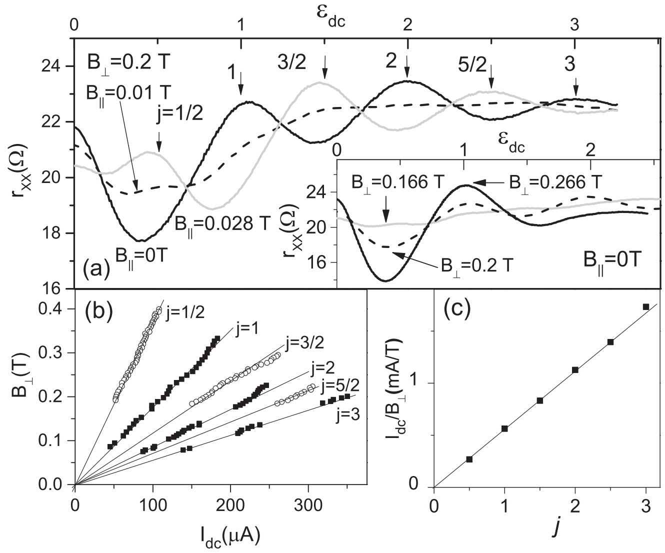

FIG. 2. (a) Dependence of differential resistance on normalized electric field, $\epsilon_{dc} = \gamma e R_c E/\hbar\omega_c$, where $\gamma = 1.9$, at different in-plane magnetic fields as labeled, obtained along the white arrow shown in Fig. 1. The inset shows the resistance evolution along the black arrow shown in the inset to Fig. 1. (b) Positions of resistance maximums shown in (a) at different magnetic fields $B_\perp$. Lines present the linear fit of the data. (c) Reciprocal slope of the linear fits shown in (b) vs index j indicating agreement with Eq. (1). Sample A.

and B with slightly different gaps, $\Delta_{12}(A) = 0.43$ meV and $\Delta_{12}(B) = 0.50$ meV, were studied.

Figure 1 presents a dependence of the resistance R_{xx} on the perpendicular magnetic field at different angles α as labeled. At $\alpha = 0^\circ$ the resistance shows low-frequency MISO (LF-MISO) and HF-MISO [38,39]. LF-MISO correspond to the scattering between the two lowest (1) symmetric and (2) antisymmetric sub-bands and obey the relation $\Delta_{12} = k\hbar\omega_c$ [40]. HF-MISO correspond to scattering between either the lowest or the third sub-band. Due to the mismatch between gaps, $\Delta_{13} - \Delta_{23} = \Delta_{12}$, HF-MISO show a beating pattern correlated with LF-MISO. In particular the nodes of HF-MISO beating are located at LF-MISO minimums. A parallel magnetic field, $B_\parallel$, moves nodes at $k = 1/2$ and $3/2$ toward each other, leading to collapse at $\alpha = 9.5^\circ$. The inset to Fig. 1 shows that odd k LF-MISO maximums are bounded by the nodal lines [40].

Figure 2 presents dependencies of the differential resistance r_{xx} on the electric field E at $B_\perp = 0.2$ T and different in-plane magnetic fields as labeled taken along the white arrow shown in the left inset to Fig. 1 [41]. At $B_\parallel = 0$ T the black solid line shows three maximums at $j = 1$, 2, and 3, which obey Eq. (1). The gray solid line presents the dependence taken at the end of the white arrow in the vicinity of the nodal line. This dependence is inverted with respect to the black line and demonstrates maximums at $j = 1/2$, $3/2$, and $5/2$. These maximums also obey Eq. (1) with the *same* fundamental periodicity $1/\hbar\omega_c$ but at the half-integer values of the index j. The dashed line presents the dependence at an intermediate field, which does not display considerable oscillations. The inset to Fig. 2 demonstrates the evolution of the electric-field induced resistance oscillations taken along the black arrow shown in Fig. 1. This evolution is due to variations of the perpendicular magnetic field, $B_\perp$, at $B_\parallel = 0$ T. These curves do not display an inversion. In contrast to the previous case at the $k = 3/2$ node the resistance oscillations cease at the fundamental frequency $(1/\hbar\omega_c)$ and only weak oscillations at second harmonics $(2/\hbar\omega_c)$ are visible. This behavior is expected. Indeed, in accordance with Eq. (2), the $k = 3/2$ LF-MISO minimum and HF-MISO node correspond to the condition $\Delta_{12} = (3/2)\hbar\omega_c$. At this condition symmetric and antisymmetric sub-band Landau levels are shifted by $3/2\hbar\omega_c$ with respect to each other and, therefore, are equally spaced by $\hbar\omega_c/2$ near the Fermi energy [40]. At $k = 3/2$ the fundamental harmonic of the density of electron states (DOS) at frequency $1/\hbar\omega_c$ is absent. Due to a small Dingle factor the amplitude of the second harmonic of the DOS is exponentially small, producing very weak geometric resonances with cyclotron orbits at frequency $\sim 2/\hbar\omega_c$ [42]. The described behavior of the DOS is valid along all nodal lines [40] so the observed inversion of resistance oscillations is intriguing.

The absence of the inversion at $B_\parallel = 0$ T suggests that the effect may have a relation to the magnetic breakdown of quasiclassical orbits [32,33,40,43–48]. Figure 3 supports this proposal. The figure presents an overall behavior of the electric-field induced resistance oscillations vs applied dc bias I_{dc} and $B_\perp$ taken at two different angles. At $\alpha = 0^\circ$ magnetic breakdown is absent [32,40] and the oscillations obey Eq. (1) with integer indices j. Solid black lines present the theoretical dependence [11,17,18]. The magnitude of the dc bias induced resistance oscillations is modulated by MISO. At LF-MISO minimum $k = 3/2$ ($B_\perp = 0.166$ T) the oscillations are almost absent (see also inset to Fig. 2) and are strongest in the vicinity LF-MISO maximums at $k = 1$ and 2. While at angle $\alpha = 9.5^\circ$ similar oscillations are seen in small $B_\perp$, the striking inversion of the oscillations is obvious at $B_\perp > 0.166$ T.

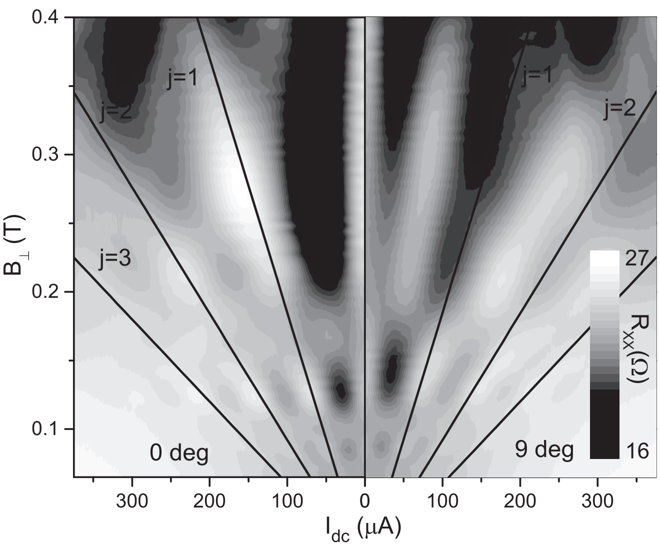

FIG. 3. Dependence of differential resistance on dc bias and $B_\perp$ at two different angles as labeled. Solid lines present dependences obtained from Eq. (1) at $\gamma = 2$ with no other fitting parameters. Sample A.

Estimations indicate a 33% probability of magnetic breakdown at $B_\perp = 0.3$ T and less than 3% at $B_\perp <= 0.166$ T [32,40].

Figure 4 presents the evolution of the dc bias induced resistance oscillations for sample B taken in the vicinity of the $k = 2$ LF-MISO maximum at $B_\perp = 0.166$ T and different $B_\parallel$. The obtained data demonstrate a reinversion of the resistance oscillations, suggesting a periodicity of the inversion with the in-plane magnetic field. Surprisingly oscillations of SdH amplitude in in-plane magnetic fields with a similar period have been recently observed (see Fig. 8 in [40]). These amplitude oscillations are related to periodic oscillations of the sub-band splitting Δ_{12} in strong magnetic fields [32,49–52].

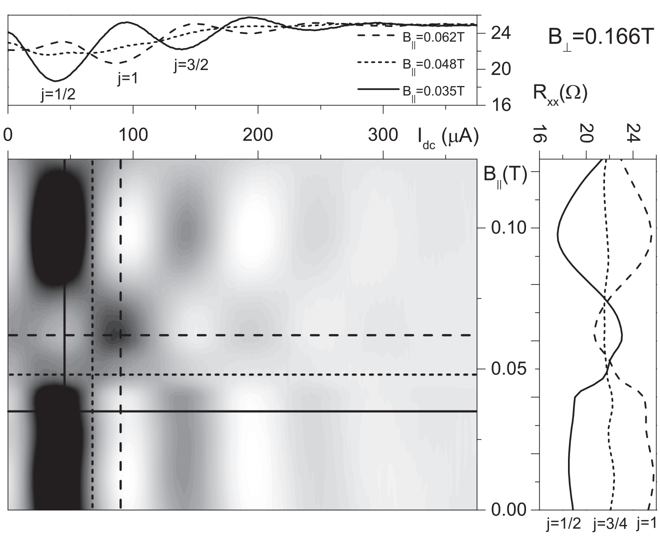

FIG. 4. Dependence of differential resistance on dc bias and in-plane magnetic fields at $B_\perp = 0.166$ T. The right panel shows reinversion of dc bias induced oscillations with in-plane magnetic field. Sample B.

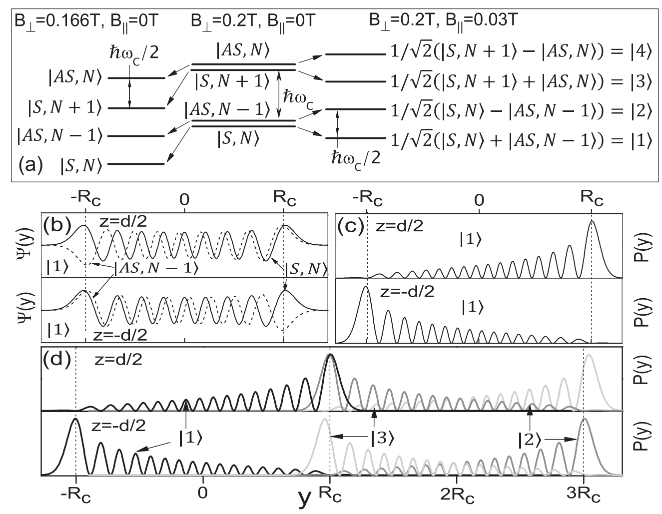

FIG. 5. (a) Evolution of energy spectra due to variation of cyclotron energy (left) and due to magnetic breakdown induced by in-plane field (right). (b) Eigenfunction $|1\rangle$ presented as a linear combination of the basis set $|\xi,N\rangle$. (c) Spatial electron distribution in the $|1\rangle$ eigenstate in top ($z = d/2$) and bottom ($z = -d/2$) 2D layers. (d) Overlap between different eigenstates during impurity backscattering.

The right panel indicates that at $j \approx 3/4$ almost no resistance oscillations are induced by $B_\parallel$. The upper panel shows that this absence of oscillations holds at $j \approx 1/4 + p/2$, where p is a positive integer.

A theory of the observed inversion of dc bias induced resistance oscillations is not available. Below, a qualitative model is proposed. Studied wide GaAs quantum wells are considered as two 2D parallel systems separated by a distance d in z direction and the coupling between the systems is treated in tight-binding approximation using a tunneling magnitude t_0 [32,40]. At $B_\parallel = 0$ T electrons occupy symmetric (S) and antisymmetric (AS) sub-bands and move in the x-y plane along cyclotron orbits with radius R_c at the Fermi energy. In $B_\perp$ the lateral electron motion is quantized and the eigenfunctions can be presented as $|\xi,N\rangle$, where $\xi = S,AS$ and $N = 0,1,2\ldots$ numerates Landau levels [40]. An application of the in-plane magnetic field $B_\parallel||E||y$ mixes the symmetric and antisymmetric states. In the vicinity of the nodal line surrounding the $k = 1$ region eigenfunctions are well approximated by a linear combination of one symmetric and one antisymmetric state (see Fig. 10 in [40]), which for simplicity of the presentation we consider to be equally populated: $|l\rangle = (|S,N{+}1\rangle \pm |AS,N\rangle)/\sqrt{2}$, where index l numerates ascending energy levels. Figure 5(a) presents an evolution of the electron spectrum along the black and white arrows shown in Fig. 1. The evolution corresponds to numerical computations of the spectrum in the vicinity of Fermi energy [40].

Resistance oscillations are observed at high filling factors and, thus, the semiclassical treatment is appropriate. It is accepted that the main contribution to dc bias induced resistance oscillations comes from electron backscattering by impurities [11,17,18]. The backscattering occurs near the turning points of the cyclotron orbits displaced by distance $2R_c$ along the electric field E. The electron spends a considerable amount of time at these points and the overlap between incident and scattered electron orbits is maximized [17,18,53,54]. Below, we analyze the spatial structure of eigenfunctions.

Figure 5(b) shows the wave function $|1\rangle = (|S,N\rangle + |AS,N\text{-}1\rangle)/\sqrt{2}$ for top $(z = d/2)$ and bottom $(z = -d/2)$ 2D layers at $N = 16$. Since N is even, the wave function $|S,N\rangle$ ($|AS,N\text{-}1\rangle$) is symmetric (antisymmetric) in both y and z directions. The eigenfunction $|1\rangle$ is a sum of these two functions that leads to the spatial electron distribution $P(y) = |\Psi(y)|^2$ shown in Fig. 5(c): at the left (right) turning point of the oscillator state $|1\rangle$ an electron is located mostly in the bottom (top) 2D layer at $-R_c$ (R_c). A similar configuration is obtained for state $|3\rangle$ while the electron distribution in state $|2\rangle$ is the distribution in state $|1\rangle$ rotated by 180° around the $y = 0$ axis.

The electric field E tilts the spectrum in y direction (not shown) that allows horizontal transitions between the levels due to elastic impurity scattering, which is considered as a local perturbation [11,17,18]. The impurity backscattering near the turning points changes the direction of electron velocity by π, which is accomplished by an overlap between the incoming state near a turning point and the outgoing state located near the *opposite* turning point of the oscillator shifted by $2R_c$. Illustrating this statement Fig. 5(d) indicates that the wave functions of the states $|1\rangle$ and $|2\rangle$ overlap at the opposite turning points, which leads to backscattering while the backscattering between states $|1\rangle$ and $|3\rangle$ is significantly suppressed since these wave functions at the opposite turning points are located in *different* 2D layers and, thus, the overlap between two functions is exponentially small. Similar consideration indicates the presence (absence) of backscattering between states $|l\rangle$ and $|m\rangle$ with different (the same) parity of indices: $\mathrm{mod}_2(m - l) = 1$ [$\mathrm{mod}_2(m - l) = 0$]. At nodal lines the energy difference between states with different index parity obeys the relation $\delta E = E_m - E_l = \hbar\omega_c(j + 1/2)$, that leads to the relation $\gamma e R_c E = \hbar\omega_c(j + 1/2)$ for the electric-field induced resistance oscillations in tilted magnetic field.

At zero dc bias the backscattering occurs inside the same quantum level. Thus in tilted magnetic fields the impurity backscattering in the linear response is suppressed at the nodal lines since the parities of the incoming and outgoing states are the same. This conclusion is in agreement with the experiment. Indeed Fig. 1 shows that at the $k = 3/2$ HF-MISO node located at $B_\perp = 0.2$T and $B_\parallel = 0.033$ T the resistance reaches a value which is *less* than the value of the resistance both at $k = 3/2$ at $B_\parallel = 0$ T and even at zero magnetic field. The data indicate that electron backscattering by impurities is effectively *controlled* by in-plane magnetic field. This result may have important implications for the field of topological insulators, where electron backscattering is considered to be crucial.

In conclusion the electric-field induced resistance oscillations are studied in wide GaAs quantum wells placed in tilted quantizing magnetic field. The oscillations are related to impurity assisted Landau-Zener transitions between quantum levels and in perpendicular magnetic fields obey the relation $2eR_cE = j\hbar\omega_c$, where j is a positive integer. A tilt of the magnetic field inverts the oscillations. The strongest inversion occurs at the nodal line of the beating between magneto-inter-sub-band resistance oscillations at which the density of electron states is nearly constant. These oscillations obey the relation $2eR_cE = j\hbar\omega_c$, where j is a positive half integer. The effect is related to spatial redistribution of eigenfunctions of multi-sub-band electron systems leading to *significant* modification of the electron backscattering in tilted magnetic fields.

This work was supported by the NSF (Division of Material Research, Grant No. 1104503), the Russian Foundation for Basic Research (Project No. 14-02-01158), and the Ministry of Education and Science of the Russian Federation.

[1] D. Shoenberg, *Magnetic Oscillations in Metals* (Cambridge University Press, New York, 1984).

[2] Sankar D. Sarma and Aron Pinczuk, *Perspectives in Quantum Hall Effects* (Wiley-VCH, Weinheim, 2004).

[3] Jing-qiao Zhang, Sergey Vitkalov, A. A. Bykov, and A. K. Kalagin, and A. K. Bakarov, Phys. Rev. B **75**, 081305(R) (2007).

[4] Jing Qiao Zhang, Sergey Vitkalov, and A. A. Bykov, Phys. Rev. B **80**, 045310 (2009).

[5] N. C. Mamani, G. M. Gusev, O. E. Raichev, T. E. Lamas, and A. K. Bakarov, Phys. Rev. B **80**, 075308 (2009).

[6] I. A. Dmitriev, M. G. Vavilov, I. L. Aleiner, A. D. Mirlin, and D. G. Polyakov, Phys. Rev. B **71**, 115316 (2005).

[7] A. A. Bykov, Jing-qiao Zhang, Sergey Vitkalov, A. K. Kalagin, and A. K. Bakarov, Phys. Rev. Lett. **99**, 116801 (2007).

[8] W. Zhang, M. A. Zudov, L. N. Pfeiffer, and K. W. West, Phys. Rev. Lett. **100**, 036805 (2008).

[9] G. M. Gusev, S. Wiedmann, O. E. Raichev, and A. K. Bakarov, and J. C. Portal, Phys. Rev. B **83**, 041306 (2011).

[10] A. A. Bykov, Sean Byrnes, Scott Dietrich, Sergey Vitkalov, I. V. Marchishin, and D. V. Dmitriev, Phys. Rev. B **87**, 081409(R) (2013).

[11] C. L. Yang, J. Zhang, R. R. Du, J. A. Simmons, and J. L. Reno, Phys. Rev. Lett. **89**, 076801 (2002).

[12] A. A. Bykov, J. Q. Zhang, S. Vitkalov, A. K. Kalagin, and A. K. Bakarov, Phys. Rev. B **72**, 245307 (2005).

[13] W. Zhang, H. S. Chiang, M. A. Zudov, L. N. Pfeiffer, and K. W. West, Phys. Rev. B **75**, 041304 (2007).

[14] A. T. Hatke, M. A. Zudov, L. N. Pfeiffer, and K. W. West, Phys. Rev. B **83**, 081301(R) (2011).

[15] A. V. Goran, A. K. Kalagin, and A. A. Bykov, JETP Lett. **94**, 535 (2011).

[16] Scott Dietrich, Sean Byrnes, Sergey Vitkalov, and A. V. Goran, and A. A. Bykov, Phys. Rev. B **86**, 075471 (2012).

[17] M. G. Vavilov, I. L. Aleiner, and L. I. Glazman, Phys. Rev. B **76**, 115331 (2007).

[18] M. Khodas and M. G. Vavilov, Phys. Rev. B **78**, 245319 (2008).

[19] P. T. Coleridge, Semicond. Sci. Technol. **5**, 961 (1990).

[20] D. R. Leadley, R. Fletcher, R. J. Nicholas, F. Tao, C. T. Foxon, and J. J. Harris, Phys. Rev. B **46**, 12439 (1992).

[21] A. A. Bykov, D. R. Islamov, A. V. Goran, and A. I. Toropov, JETP Lett. **87**, 477 (2008).

[22] A. A. Bykov, JETP Lett. **88**, 64 (2008).
[23] A. A. Bykov, JETP Lett. **88**, 394 (2008).
[24] N. C. Mamani, G. M. Gusev, T. E. Lamas, A. K. Bakarov, and O. E. Raichev, Phys. Rev. B **77**, 205327 (2008).
[25] A. A. Bykov, JETP Lett. **89**, 461 (2009).
[26] A. V. Goran, A. A. Bykov, A. I. Toropov, and S. A. Vitkalov, Phys. Rev. B **80**, 193305 (2009).
[27] L. I. Magarill and A. A. Romanov, Sov. Phys. Solid State **13**, 828 (1971).
[28] V. M. Polyanovskii, Sov. Phys. Semicond. **22**, 1408 (1988).
[29] M. E. Raikh and T. V. Shahbazyan, Phys. Rev. B **49**, 5531 (1994).
[30] O. E. Raichev, Phys. Rev. B **78**, 125304 (2008).
[31] G. S. Boebinger, A. Passner, L. N. Pfeiffer, and K. W. West, Phys. Rev. B **43**, 12673 (1991).
[32] J. Hu and A. H. MacDonald, Phys. Rev. B **46**, 12554 (1992).
[33] N. E. Harff, J. A. Simmons, S. K. Lyo, and J. F. Klem, G. S. Boebinger, L. N. Pfeiffer, and K. W. West, Phys. Rev. B **55**, R13405 (1997).
[34] G. M. Gusev, A. K. Bakarov, T. E. Lamas, and J. C. Portal, Phys. Rev. Lett. **99**, 126804 (2007).
[35] N. Kumada, K. Iwata, K. Tagashira, Y. Shimoda, K. Muraki, and Y. Hirayama, and A. Sawada, Phys. Rev. B **77**, 155324 (2008).
[36] G. M. Gusev, C. A. Duarte, T. E. Lamas, A. K. Bakarov, and J. C. Portal, Phys. Rev. B **78**, 155320 (2008).
[37] M. A. Mueed, D. Kamburov, M. Shayegan, L. N. Pfeiffer, K. W. West, K. W. Baldwin, and R. Winkler, Phys. Rev. Lett. **114**, 236404 (2015).
[38] Scott Dietrich, Jesse Kanter, William Mayer, Sergey Vitkalov, D. V. Dmitriev, and A. A. Bykov, Phys. Rev. B **92**, 155411 (2015).
[39] S. Wiedmann, G. M. Gusev, O. E. Raichev, A. K. Bakarov, and J. C. Portal, Phys. Rev. B **82**, 165333 (2010).
[40] William Mayer, Jesse Kanter, Javad Shabani, Sergey Vitkalov, A. K. Bakarov, and A. A. Bykov, Phys. Rev. B **93**, 115309 (2016).
[41] Electric field E equals Hall electric field E_H with accuracy better than 1% and the difference is ignored.
[42] The studied samples show quantum scattering time $\tau_q = 8$ ps [38,40]. This time leads to ratio $\sim 1/25$ between amplitudes of dc bias induced quantum oscillations at $k = 3/2$ ($B_\perp = 0.166$ T, $\hbar\omega_c/2$ level separation) and $k = 1$ ($B_\perp = 0.266$ T, $\hbar\omega_c$ level separation) [17,18].
[43] M. G. Priestley, Proc. R. Soc. A **276**, 258 (1963).
[44] M. H. Cohen and L. Falicov, Phys. Rev. Lett. **7**, 231 (1961).
[45] E. I. Blount, Phys. Rev. **126**, 1636 (1962).
[46] A. A. Slutskin, Sov. Phys. JETP **26**, 474 (1968).
[47] A. B. Pippard, Proc. R. Soc. A **270**, 1 (1962).
[48] A. B. Pippard, Phil. Trans. R. Soc. A **256**, 317 (1964).
[49] Perez Moses and Ross H. McKenzie, Phys. Rev. B **60**, 7998 (1999).
[50] Victor M. Yakovenko and Benjamin K. Cooper, Physica E **34**, 128 (2006).
[51] J. Wosnitza, *Fermi Surfaces of Low Dimensional Organic Metals and Superconductors* (Springer, Berlin, 1996).
[52] T. Ishiguro, K. Yamaji, and G. Saito, *Organic Superconductors*, 2nd ed. (Springer, Berlin, 1998).
[53] M. A. Zudov, I. V. Ponomarev, A. L. Efros, R. R. Du, J. A. Simmons, and J. L. Reno, Phys. Rev. Lett. **86**, 3614 (2001).
[54] S. Vitkalov, Int. J. Mod. Phys. B **23**, 4727 (2009).